Observational Analyses of Baroclinic Boundary Layer Characteristics during One Frontal Winter Snowstorm[①]

Xu Yinlong (许吟隆) P4 A

Agrometeorology Institute, Chinese Academy of Agricultural Sciences, Beijing 100081

Qian Fenlan (钱粉兰), Chen Zhi (陈 陟), Li Shiming (李诗明)
and Zhou Mingyu (周明煜)

National and Center for Marine Environmental Forecast Research, Beijing 100081

(Received January 8, 2001; revised October 22, 2001)

ABSTRACT

The evolution and characteristics of the baroclinic boundary layer for one frontal winter snowstorm were analyzed by using the well-documented dataset during Intensive Observation Period (IOP) 17 of STORM-FEST. It is found that when the warm moist air was lifted across the front, a great amount of latent heat release because of snowing increased the frontal temperature contrast to intensify frontogenesis. It is shown in the zig-zag section diagram of potential temperature that when the frontogenesis got stronger, a cold trough was formed and both low-level jet (LLJ) and upper-level jet (ULJ) emerged ahead of the front. In the strongest stage of frontogenesis, the frontal contrast of potential temperature of cold trough reached as high as 20 K. Hereafter the LLJ ahead of the front tended to weaken and the LLJ behind the front tended to strengthen. The frontal circulation system was dominated by the cold air advection behind the front, which transported the cold air behind the front forward to the warm area ahead of the front to weaken the cold trough and finally frontolysis occurred. It is shown by the analyses of turbulent characteristics of frontal baroclinic boundary-layer that the vertical shear (uw) above the boundary layer was very large, and the pumping of the strong wind shear in turbulent energy budget made the characteristic variables within the PBL well mixed. Sufficient moisture carried by southerly flow from the Mexico Gulf, and the strong baroclinity of the frontal boundary layer played key roles in this frontal winter snowstorm, and the large-scale ULJ behind the cold front is also advantageous to the development of the convective boundary layer.

Key words: STORM-FEST, Frontogenesis, Baroclinic boundary layer, Winter snowstorm

1. Introduction

The frontal atmospheric boundary layer is characterized by strong baroclinity. To study the characteristics and evolution of frontal baroclinic boundary layer is of great importance to the understanding of the mesoscale weather phenomenon. Hoxit (1974) analyzed the relationship between the variations in baroclinity (thermal wind) and the changes in the planetary boundary layer (PBL) wind profile by using the regular radiosonde data of 19 interior stations in the portions of the eastern half of the United States. Lenschow et al. (1980) evaluated the budgets of turbulent kinetic energy, temperature and humidity variances, and temperature

①This research was financially supported by the National Natural Science Foundation of China under Grant No. 49675251.

and humidity fluxes in a baroclinic convective boundary layer during the wintertime cold air outbreaks with the aircraft data of the Air Mass Transformation Experiment (AMTEX).

Because of the sparsity of observation data, it is greatly restricted to the study on the structure and characteristics of strong baroclinic PBL. From 1 February to 15 March 1992, the Storm–Scale Operational and Research Meteorology–Fronts Experiment Systems Test (STORM–FEST) was carried out in the central US to begin to document the three–dimensional structures and evolutions of the various types of fronts that affected the central United States for determining the dynamical and physical processes governing the structures and evolutions of these kinds of fronts. There were 20 IOPs done during 44 days of STORM–FEST. A frontal winter snowstorm had been completely monitored in IOP 17, which began at 1200 GMT 8 March and ended at 1200 GMT 10 March 1992 in the FEST domain. This winter snowstorm was triggered when the arctic cold front merged with a surface low moving from the west coast of US into the FEST domain, providing deep upslope conditions over the frontal range for good moist southerly low level flow ahead of the surface low. LeMone et al. (1999) presented a case study on boundary layer characteristics of a day with vertical shear in the mixed layer on 27 February and compared with a similar case with virtually no shear on 10 March in IOP 17 to isolate the mechanisms that determine the vertical shear of the horizontal wind in the convective mixed layer. In this paper, we will focus our analysis on the evolution of wind field, temperature and humidity field, to identify the relationship between frontal circulation and frontogenesis during outbreak of this winter snowstorm and the turbulent characteristics in the mixed layer following this frontal weather event.

2. Summary of observation data

All observing systems available, including surface data network, upper–air soundings, aircraft, radar, and Satellite, were operated and an unparalleled dataset on this frontal winter snowstorm was obtained during STORM–FEST IOP 17. Surface data were obtained from United States and Canadian national, regional, and research networks. Totally, there were 120 sites for 5 min resolution composite data, 720 sites for 1 h resolution composite data, and 2700 sites for hourly and 15 min precipitation composites. Almost all of surface stations were operated satisfactorily during IOP 17.

Upper–air soundings during IOP 17 consisted of the U. S. National Weather Service (NWS), Canadian Atmospheric Environment Service (AES), Cross–chain Loran Atmospheric Sounding System (CLASS), dropsonde and Profiler Systems. Besides 33 sounding stations of NWS, there were also 9 stations of Canadian AES and 12 stations of CLASS to provide standard 12 h and special 3 h and 6 h soundings data during IOP 17 at different stage of this winter snowstorm as requested by STORM–FEST operations. Higher density "Picket Fence" network consisted of a total of 15 stations along the west coast to provide observations of the environmental flow conditions upstream of the STORM–FEST domain. Twenty–six 403 MHz profilers of the NOAA Demonstration Profiler network in and near the STORM–FEST domain to collect 6 min and 1 h time resolution vertical profiles of wind and temperature from 0.5 to 14 km altitude. Five boundary–layer Profilers (915 MHz) were operated by NOAA / Wave Propagation Laboratory to measure vertical profiles of winds and temperatures at 0.5 h intervals. Radar data were also obtained by CP–3, CP–4 of NCAR Research Doppler Radar in northeastern Kansas, NSSL Cimarron Doppler Radar located at NOAA / NSLL, Illinois HOT 5 cm Wavelength Doppler Radar located at the Urban–

Champaign Airport to support intensive observation on this winter snowstorm. During 0600 GMT–1400 GMT 10 March, NOAA P–3 took off to document the characteristics of the frontal system. The flight track selected was from northwestern Arkansas to Birmingham, Alabama. On the return leg to Richards–Geaur AFB, 13 dropsondes were deployed from 22 kt to obtain additional documentation of the frontal feature. From 1600 GMT 10 March, during IOP 18 the NCAR King Air took off to investigate the sensible heat and momentum budgets in a baroclinic boundary layer. In general, all surface based and aircraft systems were operational and satisfactory dataset was obtained. Operation summary (Intensive observation operations listed only, routine observation operations are not listed) of IOP 17 is listed in Table 1 and more information about this winter snowstorm is available in STORM–FEST Operations Summary and Data Inventory (1993).

Table 1. Operation summary of IOP 17

	Network	Number of Soundings Sites	Beginning of IOP	Ending of IOP	Interval of Release
Upper Air	CLASS	12	1200 GMT 8 March	1200 GMT 10 March	3 h
	NWS (Inner)	22	1200 GMT 8 March	1200 GMT 10 March	3 h
	NWS (Outer)	11	0000 GMT 6 March	1200 GMT 9 March	6 h
	Picket Fence	9	1200 GMT 5 March	1200 GMT 7 March	3 h
	Canadian AES	9	0000 GMT 7 March	1200 GMT 9 March	6 h
Radar	Name	Operational Period			
	CP–3	1200 GMT 8 March–1700 GMT 9 March			
	CP–4	1200 GMT 8 March–1700 GMT 9 March			
	HOT	0730 GMT 7 March, 0100 GMT–2130 GMT 10 March			
	Cimarron	2300 GMT 8 March–0522 GMT 9 March			
Aircraft	NOAA P–3	0554 GMT–1519 GMT 9 March, 0600 GMT–1400 GMT 9 March			
	NCAR KA	1240 GMT–1527 GMT 9 March, 1700 GMT–2033 GMT 9 March, 2306 GMT 9 March–0142 GMT 10 March, 1732 GMT–2204 GMT 10 March*			
	UW KA	1156 GMT–1804 GMT 9 March			
	UW C–131	1842 GMT 8 March–2242 GMT 9 March			
Satellte	GOES RISOP	1200 GMT 8 March–1200 GMT 10 March			

* IOP 18

3. Synoptic summary

It can be seen from 500 hPa synoptic chart that at 1200 GMT 7 March an upper–level trough had moved onto the west coast of US, with a weak surface low analyzed over southern Arizona in surface map. Meanwhile an arctic cold front had reached North Dakota but mostly fairskies were forecasted over the STORM–FEST domain. At 1200 GMT 8 March the arctic front had invaded Nebraska, the upper level trough and cutoff low moved into the west portion of the STORM–FEST domain coincident with the low level intrusion of arctic air in the north portion of the STORM–FEST domain. A surface low in southeastern Colorado pushed eastward into Texas and Oklahoma, where the initial development of convection took place. Strong LLJ moved around this cutoff low to transport sufficient moisture from Mexico Gulf to the Texas / Oklahoma panhandle region, strong low–level flow with good turning in the low–level winds, severe snowstorm was possible. On 9 March, a deep surface low developed over southeastern Colorado and Wyoming. As the arctic front moved into Colorado, it enhanced the deep upslope conditions over the front range causing very heavy snow. By 1200 GMT 9 March, almost two feet of snow had fallen from Boulder to Ft. Collins, Colorado. Hereafter the arctic front began to move into the boundary layer domain at about 1200 GMT 10 March, this frontal winter snowstorm moved eastward and was located over the Ohio valley with a broad area of precipitation both ahead of and behind the front. When the cold front was over, the boundary layer atmosphere was characterized by strong baroclinity and the mixing layer was deep. Strong northerly winds dominated the most of the STORM–FEST domain as a 1024 hPa high pressure moved into the region (the surface maps for IOP 17 available in STORM–FEST documentation).

4. Analyses of boundary–layer characteristics

4.1 *Characteristics of wind field*

The STORM–FEST domain and the selected zig–zag section were drawn in Fig. 1. At 1200 GMT 8 March the polar arctic air began to invade the STORM–FEST domain. Corresponding to the invasion of the polar arctic air, sharp turning of wind direction, shifted from southerly in the low–level air to northwesterly in the upper–level air, was observed by the upper–air soundings in BIS and HON stations. At 0600 GMT 9 March it can be seen by the combination of changes of wind speed and directions in Fig. 2 that the cold front was situated between HON and OMA stations, and the low–level wind speed increased suddenly from 10 m s^{-1} behind the front to 20 m s^{-1} ahead of the front between OMA and 62 K station and there was a wide LLJ with wind speed of 20 m s^{-1} between 62 K and LIT stations in the level between 950 hPa and 750 hPa. From 0600 GMT to 1200 GMT 9 March the cold front continued to move into the inner STORM–FEST domain. By 1200 GMT 9 March, it can be seen from turning of wind direction (Fig. 3a) that the front had moved over the OMA station. Southwesterly ULJ with wind speed of 40 m s^{-1} emerged upper to OMA and UMN stations above 400 hPa, and the LLJ ahead of the front still existed between TOP and LIT stations. Northeasterly LLJ with wind speed of more than 20 m s^{-1} began to emerge upper to HON station at the level between 900 hPa and 800 hPa behind the front (Fig. 3b). At 1800 GMT 9 March compared with the zig–zag section diagram of potential temperature (Fig. 5c) discussed below it is shown that the frontogenesis reached its strangest stage and the jets ahead of the front also reached their maximum value (LLJ–30 m s^{-1} and ULJ–60 m s^{-1}) (Fig. 4), and the LLJ followed the front closely. It can be seen in Fig. 4 that wind directions turned from southwesterly ahead of the front to northeasterly behind the front, frontal surface was a transitional area of the minimum wind speed between the LLJ ahead of the front and the LLJ behind the front, forming a typical frontal circulation. After 1800 GMT the LLJ and ULJ ahead of the front began to weaken but the LLJ behind the front maintained until 0600 GMT 10 March. At the end time of observation, northerly wind dominated the STORM–FEST domain as a high pressure of 1024 hPa took over the STORM–FEST domain, and the ULJ with wind speed of 40 m s^{-1} existed at 400 hPa level.

4.2 *Characteristics of temperature and humidity field*

At 1200 GMT 8 March the arctic cold front was pushing through the north boundary of

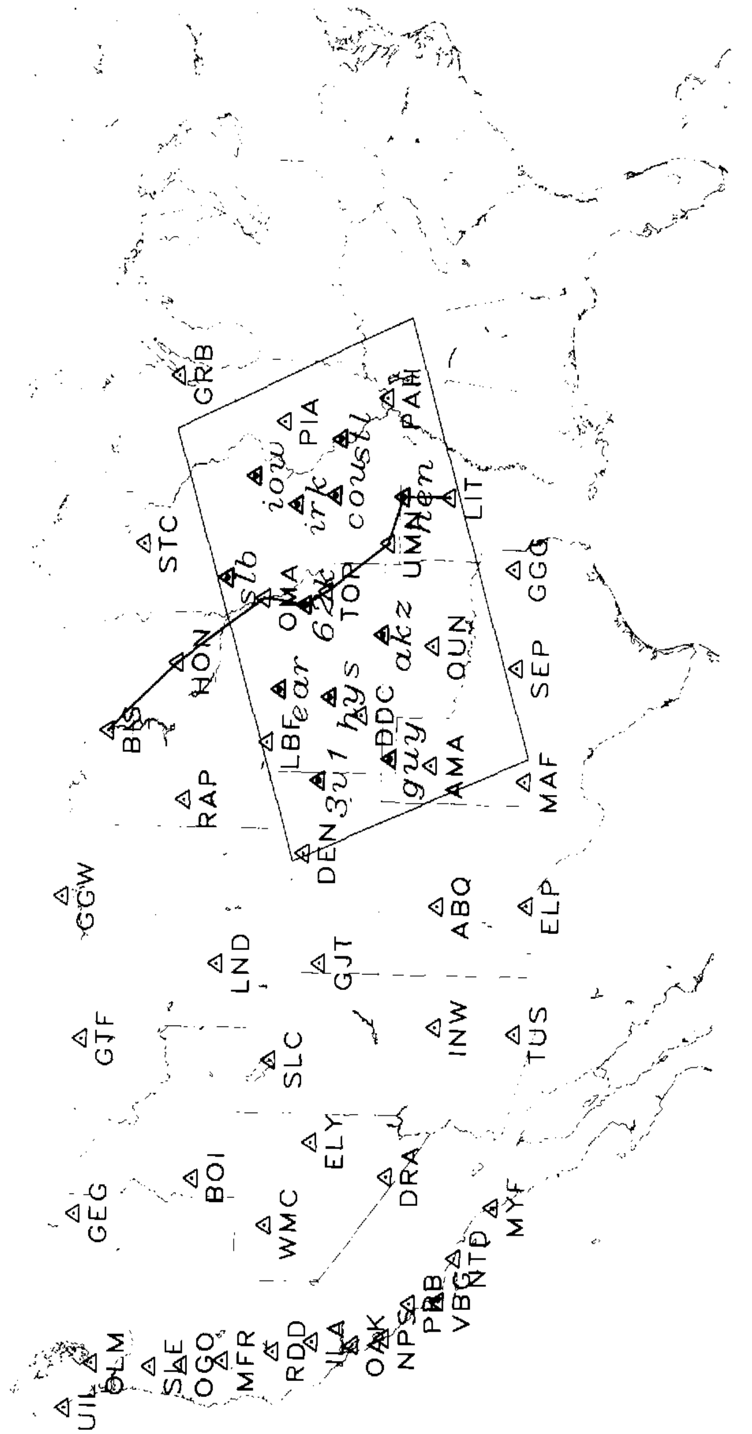

Fig. 1. STORM–FEST domain, name of upper–air sounding stations and the selected zig–zag section.

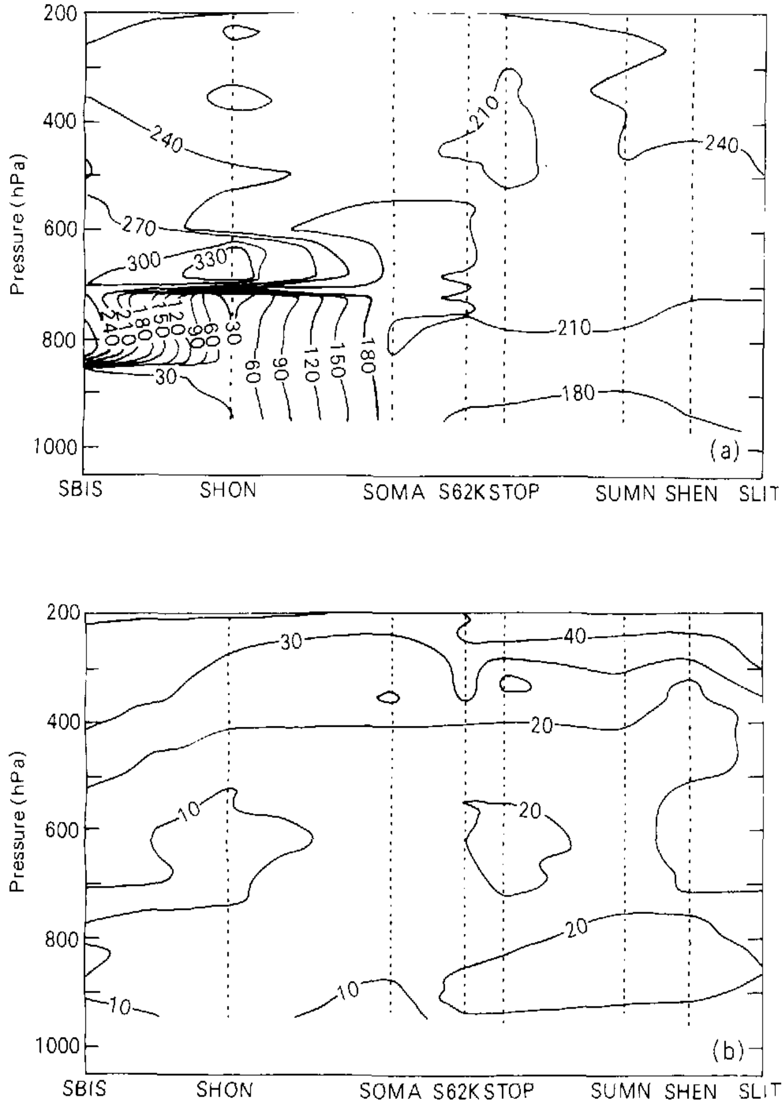

Fig. 2. Zig–zag section diagram of wind direction and speed at 0600 GMT 9 March 1992. (a) Wind direction, isoline contour: 30°; (b) Wind speed, isoline contour: 10 m s^{-1}.

the STORM–FEST domain. It is shown in Fig. 5a that at 0600 GMT 8 March the isoline of potential temperature intensified and the horizontal gradients of potential temperature obviously increased between HON and OMA stations, indicating that the cold front had moved forward and the frontogenesis enhanced. At 1200 GMT 9 March a cold tongue formed near the OMA station (Fig. 5b); at 1800 GMT 9 March (Fig. 5c) the cold tongue developed to its maximum contrast (20 K) of potential temperature, and the isoline of potential temperature near 62 K station was extremely intense. It is indicated in Fig. 5f that the isoline of mixing ratio

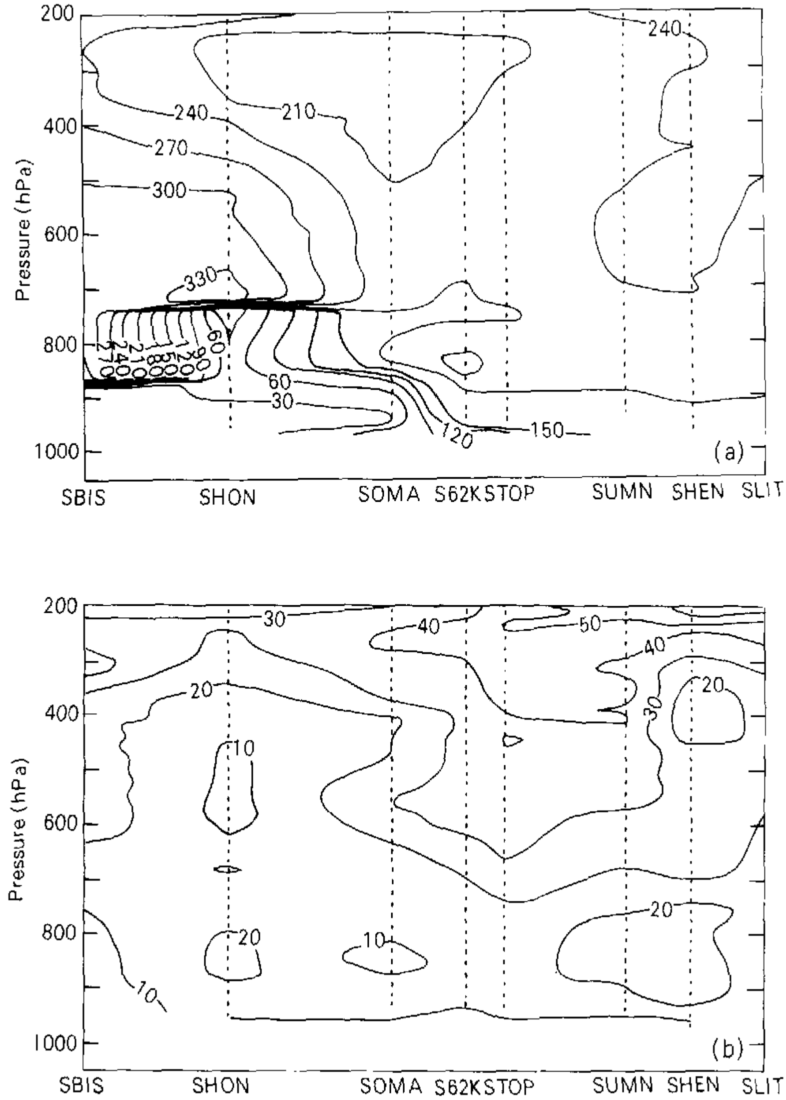

Fig. 3. Zig-zag section diagram of wind direction and speed at 1200 GMT 9 March 1992. (a) Wind direction, isoline contour: 30°; (b) Wind speed, isoline contour: 10 m s^{-1}.

of water vapor was presented with "S"–shape corresponding to the cold tongue, i. e., the large value of mixing ratio extended backward behind the front above and the small value of mixing ratio extended forward ahead of the front. For example, the isoline of 4 g kg^{-1} stretched over both OMA and 62 K stations. After 1800 GMT the cold tongue gradually decreased and the intensity of potential temperature isoline became thin as moving eastward. At 0000 GMT 10 March (Fig. 5d), the cold front moved into the region between TOP and UMN stations and the cold tongue faded away, and intensity of potential temperature isoline also became

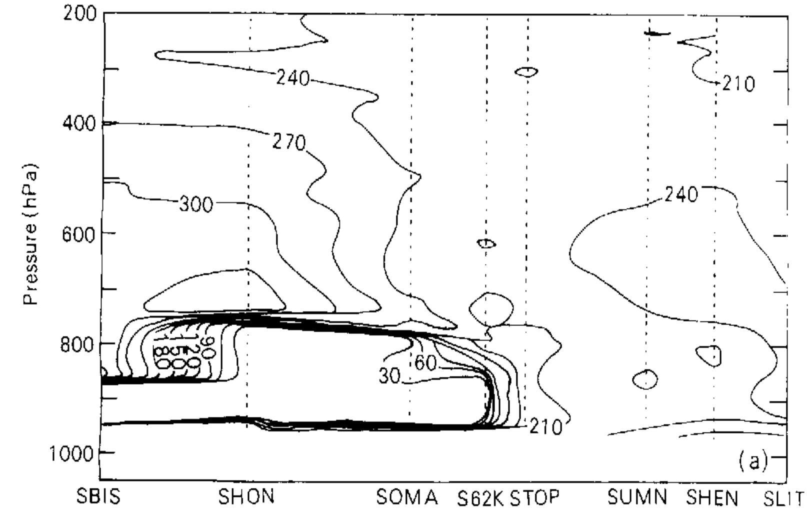

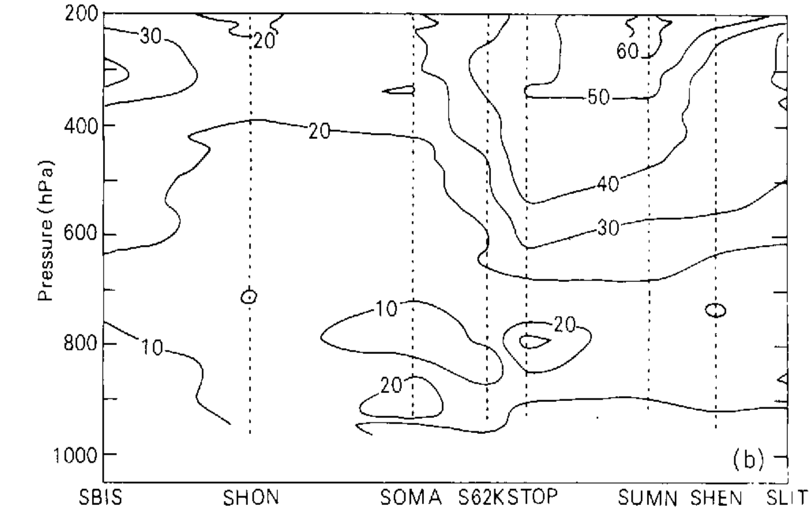

Fig. 4. Zig-zag section diagram of wind direction and speed at 1800 GMT 9 March 1992. (a) Wind direction, isoline contour: 30°; (b) Wind speed, isoline contour: 10 m s^{-1}.

thinner than at 1800 GMT 9 March, which meant that the evolution of the front was dominated by frontolysis. By 1200 GMT 10 March (Fig. 5e) the potential temperature field was horizontally homogeneous between BIS and 62 K stations, but the values of the potential temperature in the low-level atmosphere had significantly dropped, for example, the potential temperature at 950 hPa level in OMA station had dropped from 288 K to 268 K, but the influence of frontogenesis had not completely faded away between 62 K and LIT stations. It demonstrated in Fig. 5f that the isoline of mixing ratio was typical " S" -shape around the

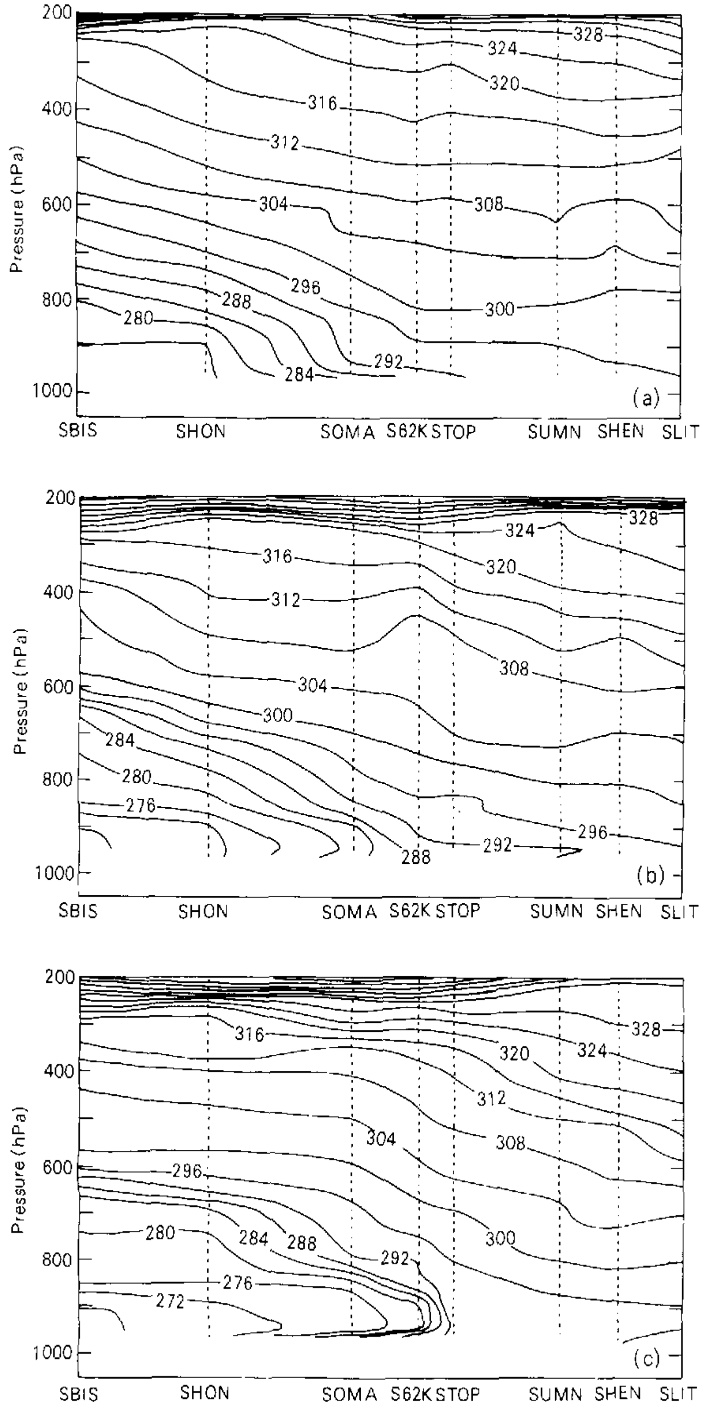
(a)
Pressure (hPa)
200
400
600
800
1000
328
324
320
316
312
308
304
300
296
292
288
284
280
SBIS SHON SOMA S62K STOP SUMN SHEN SLIT
(b)
Pressure (hPa)
200
400
600
800
1000
328
324
320
316
312
308
304
300
296
292
288
284
280
276
SBIS SHON SOMA S62K STOP SUMN SHEN SLIT
(c)
Pressure (hPa)
200
400
600
800
1000
328
324
320
316
312
308
304
300
296
292
288
284
280
276
272
SBIS SHON SOMA S62K STOP SUMN SHEN SLIT

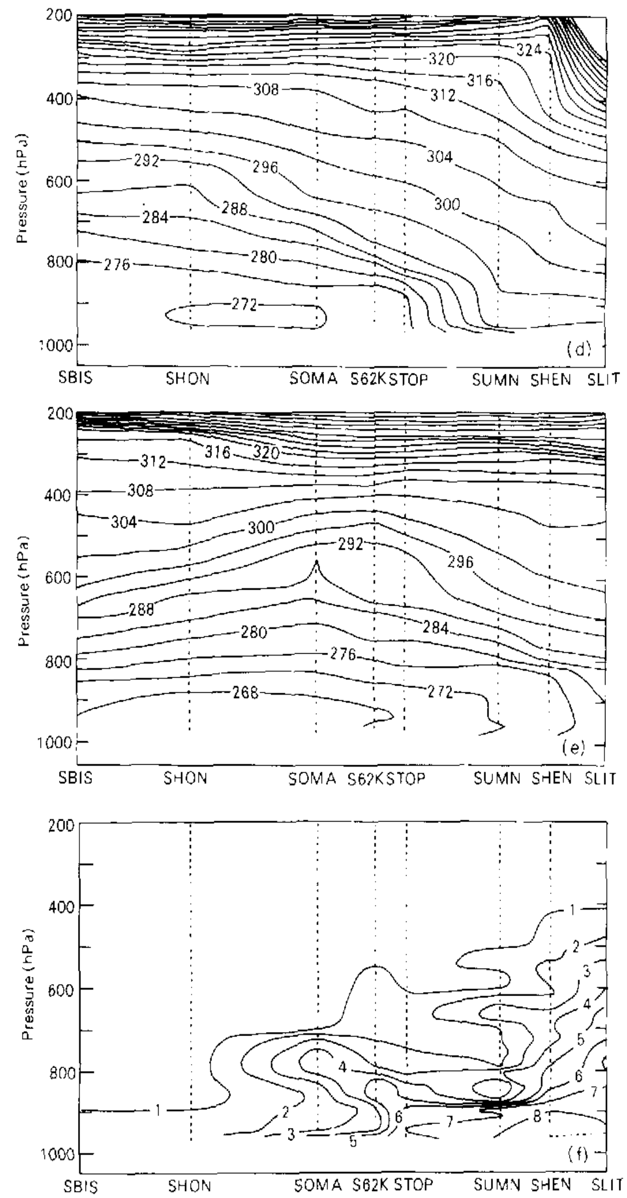

Fig. 5. Zig–zag section diagram of potential temperature, humidity (isoline contour, θ: 4 K, and q_v : 1 g kg^{-1}). (a) θ, 0600 GMT 8 March; (b) θ, 1200 GMT 9 March; (c) θ, 1800 GMT 9 March; (d) θ, 0000 GMT 10 March; (e) θ, 1200 GMT 10 March; (f) q_v , 1800 GMT 9 March.

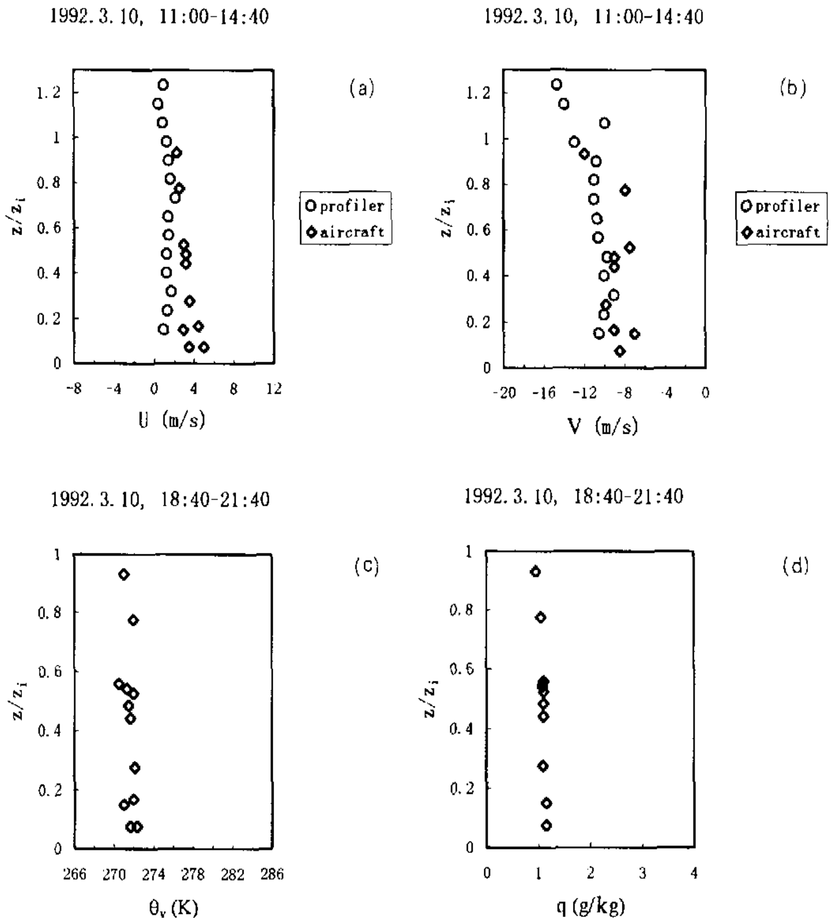

Fig. 6. Vertical distribution of (a) U, (b) V, (c) virtual potential temperature and (d) humidity on 10 March 1992.

frontal region. It can be imagined that sufficient warm moist air met the cold front to be lifted in the STORM–FEST domain, the dew–point temperature dropped suddenly and the warm moist air was condensed as cloud to produce precipitation behind the front. During the process of condensation, a great amount of latent heat was released to increase the frontal potential temperature contrast and to intensify the frontogenesis, but the upper air above the front was less affected by the cold front in a short time so that the content of water vapor was maintained at the original distribution. That is why the mixing ratio demonstrated with "S"–shape around the front.

4.3 *Characteristics of turbulent variables*

In the analyses by LeMone et al. (1999), the fair–weather convective PBL well developed

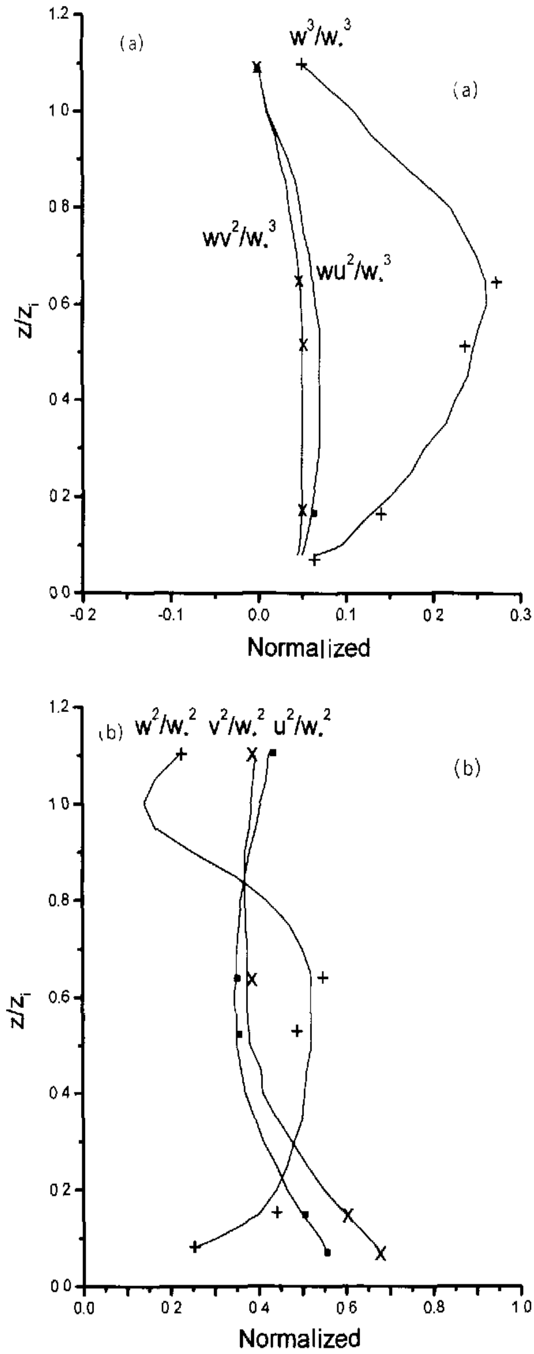

Fig. 7. Normalized vertical profiles of (a) wu^2/w_*^3, wv^2/w_*^3 and w^3/w_*^3 (b) u^2/w_*^2, v^2/w_*^2 and w^2/w_*^2 on 10 March 1992.

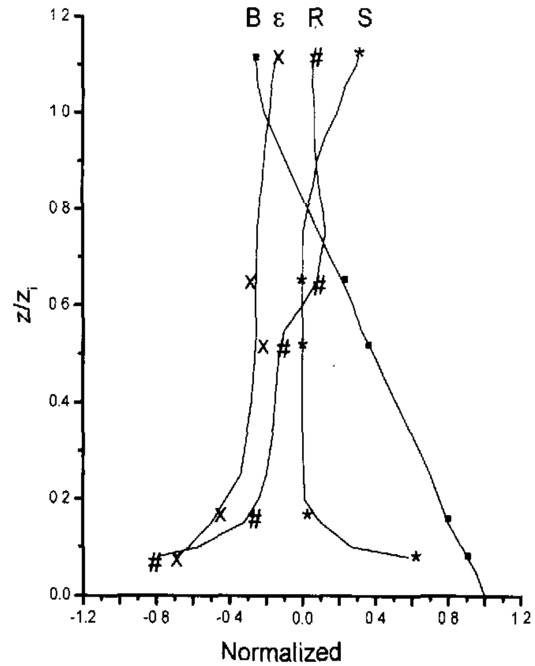

Fig. 8. Vertical distribution of turbulent energy budget B–Buoyancy production term, R–Turbulence and pressure transport term, S–Shear production term, ε–Molecular dissipation term.

in the STORM–FEST domain on 10 March but it is shown in Figs. 5d–e that the PBL was characterized by strong baroclinity. The vertical distributions of PBL characteristic variables probed by profilers and aircraft were demonstrated in Fig. 6. Within the mixed layer the variables of U, V, θ_v and q were nearly constant; however, the value of V obviously increased above the PBL. Figure 7 depicted the vertical profiles of two–order moment of U, V and W and their flux (third–order moment) within the PBL. Generally speaking, u^2 / w_*^2 and v^2 / w_*^2 (where w_* is the convective velocity) in convective PBL change greatly near the top of PBL, where the maximum values often appear, and decrease to zero with decline of the entrainment effect above the PBL. Moreover the maximum of w^2 / w_*^2 occurs at the middle of the convective PBL and the value of w^2 / w_*^2 declines with height at the upper level of PBL and approaches to zero at the top of PBL. It is shown in Fig. 7b that u^2 / w_*^2, v^2 / w_*^2 and w^2 / w_*^2 maintained large values above the top of PBL ($Z / Z_i = 1.1$, where Z is the height of PBL and Z_i is the mixing depth of PBL). In the result analyzed by Lenschow et al. (1980) with the aircraft data during AMTEX, the maximum value of w^3 / w_*^3 occurred at the height of $Z / Z_i = 0.3$. Moeng and Sullivan (1994) reported their analyses with the

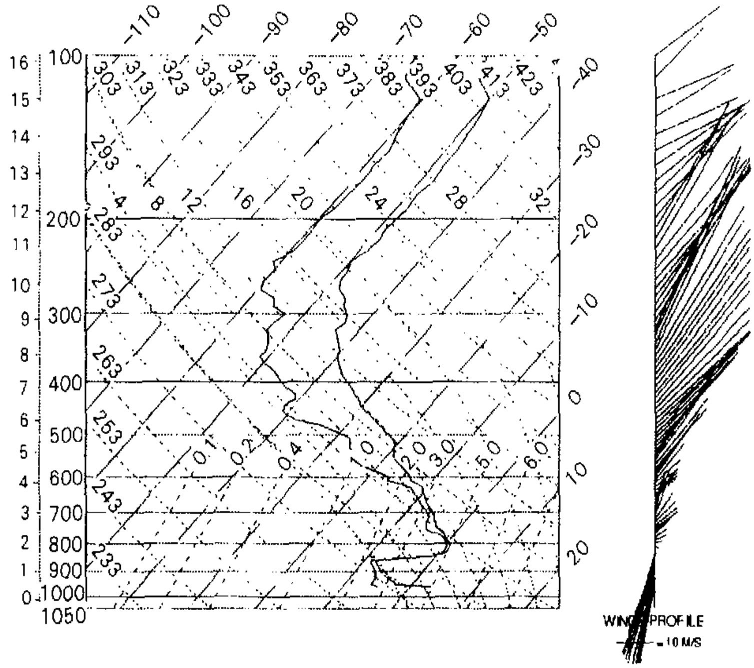

Fig. 9. Sounding profiles of wind, temperature and humidity at 62K station on 9 March 1992.

method of large eddy simulation (LES) that the maximum value of w^3/w_*^3 occurred at most at the height of $Z/Z_i = 0.5$ for the convective PBL driven only by buoyancy. However in this experiment the maximum value of w^3/w_*^3 occurred at the height of $Z/Z_i = 0.65$ (Fig. 7a), indicating that the PBL atmosphere in this experiment was more advantageous to the development of convection than that driven only by thermal forcing. It is clearly indicated that in addition to the thermal forcing, the large−scale weather system was also advantageous to the mixing of convection within PBL. It can be seen from the turbulent energy budget in Fig. 8 that the shear term (S) was very strong above the top of PBL, demonstrating that there was a fierce change of wind above the PBL. The observation of NOAA P−3 showed that there was, in strictly meaning, a ULJ above the PBL. This ULJ produced so−called pumping effect so that the vertical motion within PBL became stronger, the V−motion of momentum, vertical flux of variance were also well transported upward and make the frontal PBL atmosphere better mixed than that driven only by thermal forcing.

5. Conclusions and discussion

We can conclude from the analyses above that the arctic front merged with the surface low in the STORM−FEST domain to form strong unstable baroclinic conditions in PBL over the frontal region, and the frontal winter snowstorm was triggered when the good moist air flowed from the Mexico Gulf. At the initial stage of the winter snowstorm, the frontal circulation was dominated by the southwesterly airflow from the Mexico Gulf and the warm moist airflow was lifted across the front to produce snow. Frontogenesis intensified due to a great amount of latent heat released by snow. LLJ and ULJ occurred ahead of the front after 6 hours and 12 hours of snowing respectively. At 1800 GMT 9 March, the frontogenesis reached its strongest stage, the LLJ with more than 20 m s^{-1} emerged behind the front and a huge cold tongue of potential temperature intruded into the warm area. The contrast of potential temperature of the cold tongue reached as high as 20 K (Fig. 5c). The wind and temperature profiles observed in 62K station (Fig. 9) where the cold tongue occurred showed that between 900 hPa and 850 hPa there was an inversion layer of 10°C, within this layer the temperature profile coincided with dew–point temperature (RH–100%), wind direction turned from northeasterly LLJ (20 m s^{-1}) to southwesterly ULJ (more than 40 m s^{-1}). At this moment the LLJ behind the front began to dominate the cold advection, which transported the cold air behind the front forward to the warm area ahead of the front to weaken the cold tongue and frontolysis occurred. On 10 March the boundary–layer was still characterized by strong baroclinity when this frontal winter snowstorm moved out of the STORM–FEST domain. Analyses of turbulent variables reveal that the pumping of the large–scale ULJ above PBL made the turbulent variables within the PBL well mixed, it was advantageous to the development of baroclinic mixing layer. u^2/w_*^2, v^2/w_*^2 and w^2/w_*^2 maintained large values above the PBL, and the maximum value of w^2/w_*^2, occurred at height of $Z/Z_i = 0.65$, higher than that of the thermal convective layer driven only by buoyancy.

The following conclusions can be obtained through the above analyses:

(1) The latent–heat release of snowing increased the frontal temperature contrast, which is a main factor to the frontogenesis;

(2) At the initial stage of frontogenesis the LLJ ahead of the front dominated the frontal circulation system, and this LLJ enhanced the frontogenesis;

(3) At the strongest stage of frontogenesis, the contrast of potential temperature reached as high as 20 K. Hereafter the LLJ behind the front began to take advantage of the frontal circulation system, this cold air advection weakened the frontal contrast of potential temperature and played an important role in frontolysis;

(4) It is indicated from the turbulent energy budget in convective baroclinic PBL when the cold front faded away that the wind shear term was very strong above the PBL, the large–scale pumping in upper–air was advantageous to development of convective baroclinic PBL.

It is just a primary attempt to analyze the observational data during the STORM–FEST IOP 17 in this paper. It is found in our analyses that the latent–heat release of snowing, frontogenesis and frontal circulation interacted with each other. However, Further study is needed on the effects of latent heat on frontogenesis and LLJ, the interaction between the wind–shear and latent–heat releasing, and the interaction between the ULJ, frontal circulation and boundary layer turbulence.

The authors are grateful to Dr M. A. LeMone in the National Center for Atmospheric Research, the United States, for providing the data of STORM–FEST.

REFERENCES

Hoxit, L. R., 1974: Planetary boundary layer winds in baroclinic conditions. *J. Atmos. Sci.*, **31**, 1003–1020.

LeMone, M. A., M. Zhou, C. -H. Moeng, D. H. Lenschow, L. J. Miller, and R. L. Grossman, 1999: An observational study of wind profiles in the baroclinic convective mixed layer. *Bound.-Layer Meteor.*, **90**, 47–82.

Lenschow, D. H., J. C. Wyngaard, and W. T. Pennell, 1980: Mean-field and second-momentum budgets in a baroclinic, convective boundary layer. *J. Atmos. Sci.*, **37**, 1313–1326.

Moeng, C. -H., and P. P. Sullivan, 1994: A comparison of shear- and buoyancy-driven planetary boundary layer flows. *J. Atmos. Sci.*, **51**, 999–1022.

STORM-FEST Operations Summary and Data Inventory, 1993: Prepared by John B. Cunning, National Oceanic and Atmospheric Administration, U. S. Weather Research Program, and Steven F. Williams, UCAR Office of Field Project Support, 389pp.

一次冬季锋面暴风雪天气过程的斜压边界层特征的观测分析

许吟隆　　钱粉兰　　陈　陟　　李诗明　　周明煜

摘　要

对 STORM-FEST IOP 17 一次冬季锋面暴风雪天气过程的斜压边界层结构演变及特征进行了分析。发现:暖湿空气沿锋面抬升凝结成云,产生降水过程中释放的大量潜热显著增加锋两侧的水平温度差异,产生锋生。与锋生相伴,在锋前产生低空急流和高空急流。当锋生至最强时,锋两侧温差可达 20 K,锋前低空急流开始减弱,锋后低空急流增强,锋后冷平流开始主导锋两侧的环流系统。该冷平流削弱锋两侧的温度水平梯度,产生锋消作用。对这次锋面斜压对流边界层的湍流特征分析表明:在边界层之上切应力wv明显增大;湍能收支分析表明在边界层之上的风切变产生项很强,即大尺度天气系统有利于斜压对流边界层的发展,边界层内各量充分混合。这次冬季锋面暴风雪天气过程,冷锋前的低空南风急流从墨西哥湾携带来的充足水汽及锋区边界层大气的强斜压性是其产生的关键因子;冷锋过后,大尺度高空急流的作用更有利于对流边界层的充分发展。

关键词: STORM-FEST,锋生,斜压边界层,冬季暴风雪